Multiwavelet based Tomographic Image Denoising using New Sub-Band Adaptive Bivariate Shrinkage

[1]Mohammed Gulam Ahamad, [2]Faisal Ahamad, [1]Abdullah Aljuma and [4]Syed Amjad Ali

[1]College of Computer Engineering and Science,
Alkharj University, Saudi Arabia.
[2]Ayaan College of Engineering, Hyderabad, India
[4]Dept of ECE, Lords Institute of Engineering and Technology, India

Abstract

In order to improve the quality of an Image, a new Bivariate shrinkage is developed. Here statistical dependencies between adjacent multiwavelet coefficients is taken into account. A new non-gaussian model is formulated to characterize the dependency between a coefficient and its parent and corresponding bivariate Maximum a Posteriori (MAP) estimator is derived based on multiwavelet coefficients of a noisy image. Multiwavelets are wavelets with several scaling functions and they offer simultaneously orthogonality, symmetry and short support which is not possible with ordinary wavelets. These properties makes wavelet more suitable for Image denoising.

In this paper, new Brivariate shrinkage function in combination with Multiwavelets for Image denoising is presented and compared with other denoising techniques. Simulations reveal that the proposed methodology out performs the existing wavelet shrinkage functions.

Introduction

Our aim is to improve the quality of an image by reducing noise and at the same time preserve the actual features of an image. Here we considered Medical Tomographic image (Phantom) corrupted by additive white Gaussian noise. Multiwavelet transforms are applied on an image to obtain multiwavelet coefficients, and these coefficients are strongly dependent on each other. We proposed a new denoising algorithm using sub-band adaptive bivariate shrinkage. It is a low complex denoising algorithm which uses joint statistics of multiwavelet coefficient of Tomographic image. A new non-gaussian model is used to characterize the dependency between a child coefficient and parent coefficient and bivariate maximum a posteriori (MAP)

estimator is derived based on multiwavelet coefficients of a Noisy Tomographic image, under Bayesian frame work.

Multiwavelets are wavelets with several scaling functions and they offer simultaneously, orthogonality, symmetry and short support, which is not possible with ordinary wavelets.

These properties make multiwavelets more suitable for denoising. The filter banks in multiwavelets are matrix valued, so the input image to it must be in matrix (vector) form. But the input image is scalar form, to convert from scalar to vector form, prefiltering is used and after decomposition and denoising, post filtering is done to get back the denoised image in scalar form.

Theory and formulation of Bivariate Shrinkage Function

Here statistical dependencies between adjacent multiwavelet coefficient is taken into account.

Let w_2 be parent multiwavelet coefficient and

w_1 be child multiwavelet coefficient.

w_2 is the multiwavelet coefficient at the same position as w_1, but at the   next coarser scale

$$\left.\begin{array}{l} y_1 = w_1 + n_1 \\ y_2 = w_2 + n_2 \end{array}\right\} \tag{1}$$

Where

n_1 and n_2 are noise samples.

y_1 and y_2 are noisy observations.

We can write as,
$$y = w + n \tag{2}$$

where

$$\boldsymbol{w} = (w_1 + w_2)$$

$$\boldsymbol{y} = (y_1 + y_2)$$

and

$$\boldsymbol{n} = (n_1 + n_2)$$

The standard maximum a posteriori estimator for $\boldsymbol{w}$, given the noisy observation $\boldsymbol{y}$ is

$$\hat{w}(y) = \arg\max_{w} p_{w/y}(w/y) \tag{3}$$

$$\hat{w}(y) = \arg\max_{w}[p_{y/w}(y/w).p_{w}(w)] \tag{4}$$

$$= \arg\max_{w}[p_{n}(y-w).p_{w}(w)] \tag{5}$$

Equation (4) and (5) allow us to write estimates in terms of pdf of noise $p_{n}(n)$ and pdf of multiwavelet coefficients $p_{w}(w)$. Both pdf are necessary to estimate original signal.

Noise is assumed as identically independent distributed (i.i.d) white Gaussian. The noise pdf can be written as,

$$p_{n}(n) = \frac{1}{2\pi\sigma_{n}^{2}}\exp\left(-\frac{n_{1}^{2}+n_{2}^{2}}{2\sigma_{n}^{2}}\right) \tag{6}$$

In order to observe, pdf of multiwavelet coefficients $p_{w}(w)$, we use the joint empirical child-parent coefficients. It is hard to find a model for this pdf, but we propose the following pdf,

$$p_{w}(w) = \frac{3}{2\pi\sigma^{2}}\exp\left(-\frac{3}{\sigma}\sqrt{w_{1}^{2}+w_{2}^{2}}\right) \tag{7}$$

Here w_{1} and w_{2} are uncorrelated, but not independent. This is circularly symmetric pdf. The plot of this pdf and its contour plot is shown in Fig (1).

The MAP estimator given in eq. (5) is equivalent to,

$$\hat{w}(y) = \arg\max_{w}[\log(p_{n}(y-w)+\log(p_{w}(w)] \tag{8}$$

Let

$$f(w) = \log(p_{w}(w)$$

By using equation (6), equation (8) becomes as

$$\hat{w}(y) = \arg\max_{w}[-\frac{(y_{1}-w_{1})^{2}}{2\sigma_{n}^{2}}-\frac{(y_{2}-w_{2})^{2}}{2\sigma_{n}^{2}}+f(w)] \tag{9}$$

If $p_{w}(w)$ is assumed to be strictly convex and differentiable

$$\frac{y_{1}-\hat{w}_{1}}{\sigma_{n}^{2}}+f_{1}(\hat{w})=0 \tag{10}$$

$$\frac{y_2 - \hat{w}_2}{\sigma_n^{\;2}} + f_2(\hat{w}) = 0 \tag{11}$$

Where $f_1(\hat{w})$ and $f_2(\hat{w})$ represent the derivative of $f(w)$ with respect to w_1 and w_2 respectively.

MAP estimator corresponding to our new model given by eq. (7) can be found as,

$$\log p_w(w) = \log\left[\frac{3}{2\pi\sigma^2}.\exp\left(-\frac{3}{\sigma}\sqrt{w_1^2 + w_2^2}\right)\right]$$

$$f(w) = \log\frac{3}{2\pi\sigma^2} - \frac{3}{\sigma}\sqrt{w_1^2 + w_2^2} \tag{12}$$

From this,

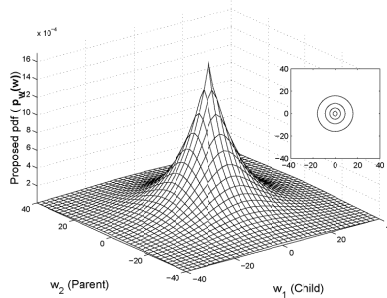$$f_1(w) = -\frac{3w_1}{\sigma\sqrt{w_1^2 + w_2^2}} \text{ and}$$

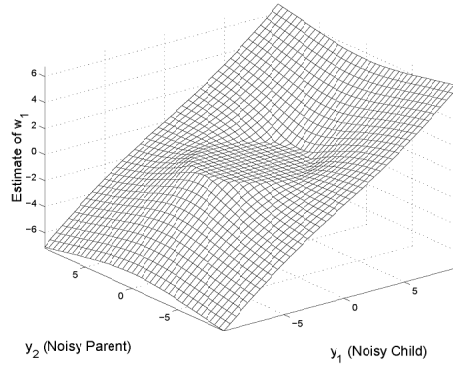$$f_2(w) = -\frac{3w_2}{\sigma\sqrt{w_1^2 + w_2^2}} \tag{13}$$

Solving equation (10) and (11) by using equation (13), the MAP estimator or the joint shrinkage function, can be written as,

$$\hat{w}_1 = \frac{\left(\sqrt{y_1^2 + y_2^2} - \frac{3\sigma_n^{\;2}}{\sigma}\right)_+}{\sqrt{y_1^2 + y_2^2}} y_1 \tag{14}$$

A plot of bivariate shrinkage function is shown in fig (2). This plot shows a circular dead zone. Our estimated value depends on parent value (y_2). The smaller the parent value, the greater the shrinkage.

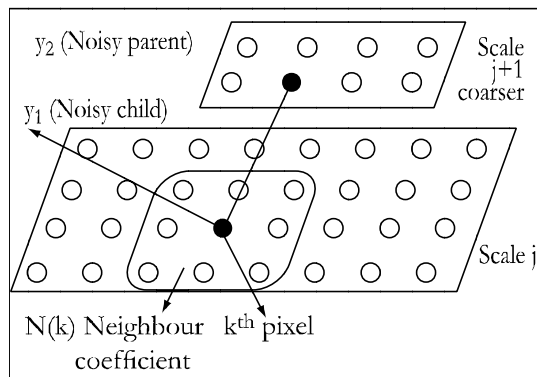**Figure 1:** New bivariate pdf proposed for joint pdf of parent-child multi wavelet coefficient pairs.

Figure 2: New bivariate shrinkage function derived from the pdf proposed.

Equation (14) can be interpreted as a bivariate shrinkage function.
It is defined as

$$(g)_+ = \begin{cases} 0, & if\ g < 0 \\ g, & otherwise \end{cases} \tag{15}$$

This estimator requires the prior knowledge of the noise variance σ_n^2 and marginal variance σ^2 for each multiwavelet coefficient. In our algorithm, the marginal variance for the kth coefficient will be estimated using neighbouring coefficients in the region $N(k)$. Here $N(k)$ is defined as all coefficients within a square-shaped window that is centered at the kth coefficient, as illustrated in fig 3.

Figure 3: Illustration of neighborhood window N(k).

To estimate the noise variance σ_n^2 from the noisy multiwavelet coefficients, a robust median estimator is used from the finest scale multiwavelet coefficients

$$\hat{\sigma}_n^{\,2} = \frac{median(|\,y_{ij}\,|)}{0.6745}, y_{ij} \in \text{ sub-band } HH_1 \tag{16}$$

To estimate the marginal variance σ^2 for the Kth multiwavelet coefficient

$$\sigma_y^{\,2} = \sigma^2 + \sigma_n^{\,2} \tag{17}$$

Where $\sigma_n^{\,2}$ is the marginal variances of noisy observations y_1 and y_2. Since y_1 and y_2 are nodded as zero mean, $\sigma_n^{\,2}$ can be found empirically by

$$\hat{\sigma}_y^{\,2} = \frac{1}{M} \sum_{y_i \in N(k)} y_{ij}^2 \tag{18}$$

Where M is the size of the neighborhood coefficient $N(k)$

$$\hat{\sigma}^2 = \hat{\sigma}_y^{\,2} - \hat{\sigma}_n^{\,2}$$

$$\hat{\sigma} = \sqrt{\left(\hat{\sigma}_y^{\,2} - \hat{\sigma}_n^{\,2} \right)} \tag{19}$$

Algorithm can be summarized as,

Calculate the noise variance $\hat{\sigma}_n^{\,2}$ using equation (16).

For each multiwavelet coefficient ($k = 1 \dots$ number of multiwavelet coefficients)

Calculate $\hat{\sigma}_y^{\,2}$ using equation (18)

Calcualte $\hat{\sigma}$ using equation (19)

Estimate each coefficient using $\hat{\sigma}$ and $\hat{\sigma}_n^{\,2}$ in equation (14).

Multiwavelets

Multiwavelets are wavelets with several scaling functions and they offer simultaneous orthogonality, symmetry and short support, which is not possible with scalar wavelets this property makes multiwavelets more suitable for various signal processing applications especially denoising.

In multiwavelet transform, filter banks are matrix valued which require two or more input streams, which can be accomplished by prefiltering.

In a general Multiresolution analysis (MRA) of multiplicity r, the scaling functions $\phi_1, \dots \phi_r$ and the corresponding multiwavelet $\psi_1, \dots \psi_r$ are usually written as vectors.

$$\Phi(t) = \left[\phi_1(t), \phi_2(t), \dots, \phi_r(t) \right]^T \tag{20}$$

Where Φ is called the multiscaling function

$$\Psi(t) = \left[\psi_1(t), \psi_2(t), ..., \psi_r(t)\right]^T \tag{21}$$

Where Ψ is called the multiwavelet function.

The dilation (scaling) and wavelet equations for multiwavelets can be written as

$$\Phi(t) = \sum_k C_k \Phi(2t - k) \tag{22}$$

$$\Psi(t) = \sum_k D_k \Phi(2t - k) \tag{22}$$

Low pass filter "C_k" and high pass filter "D_k" are $r \times r$ matrix filters. Because of extra degree of freedom, these filter coefficient provides orthogonality, symmetry, short support and high approximation order.

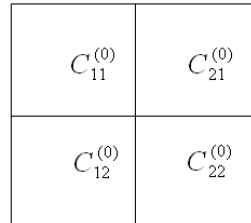Here L is chosen to be two.

Figure 4a: Original Image   **Figure 4b:** Prefiltered Image.
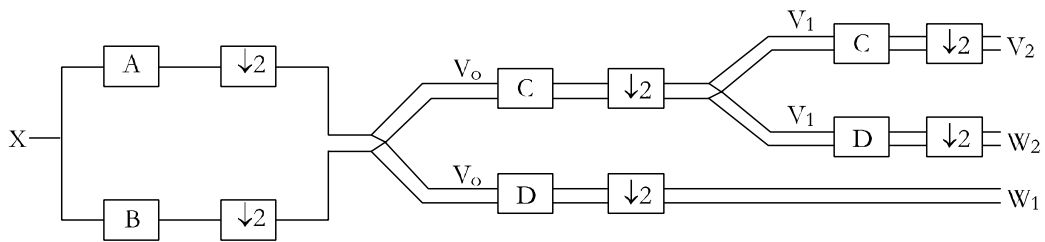

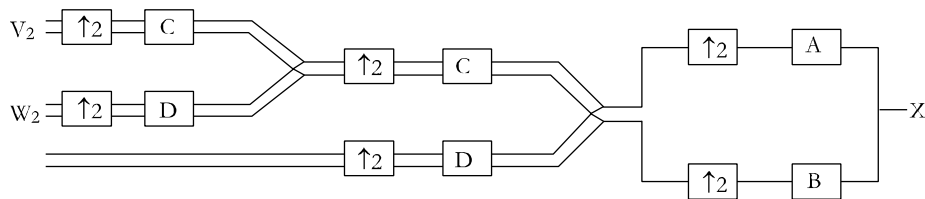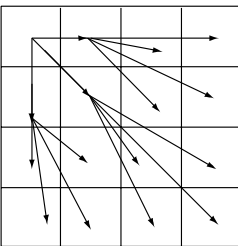**Figure 5(a):** Implementation of multiwavelet decomposition with filterbanks and repeated row prefilter.

Figure 5(b): Implementation of multiwavelet reconstruction with filterbanks and repeated row post filter.

L₁L₁	L₁L₂	L₁H₁	L₁H₂
L2L1	L₂L₂	L₂H₁	L₂H₂
H₁L₁	H₁L₂	H₁H₁	H₁H₂
H₂L₁	H₂L₂	H₂H₁	H₂H₂

Figure 6: Subbands corresponding to a single-level multiwavelet decomposition.

Figure 7: HH subband corresponding to a single-level multiwavelet decompostion.

$$\phi = \begin{bmatrix} \phi_1(t) \\ \phi_2(t) \end{bmatrix} = \sum_{k=0}^{3} C_k \begin{bmatrix} \phi_1(2t-k) \\ \phi_2(2t-k) \end{bmatrix}$$

$$\psi = \begin{bmatrix} \psi_1(t) \\ \psi_2(t) \end{bmatrix} = \sum_{k=0}^{3} D_k \begin{bmatrix} \phi_1(2t-k) \\ \phi_2(2t-k) \end{bmatrix}$$

Figure 8: Subband relation.

Reasons for choosing multiwavelets

1. The extra degree of freedom inherent in multiwavelets can be used to reduce restrictions on the filter properties. Wavelets do not have simultaneously both orthogonality and symmetric impulse response, that has length greater than 2. Symmetric filters are necessary for symmetric signal expansion, while orthogonality makes the transform easier to design and implement.
2. Longer filter lengths are required to achieve higher order of approximation, which is desired for better coding gain.
3. Short wavelet support is generally preferred to achieve a better localized approximation of the input function.
4. A better energy compaction is achieved with multiwavelets. A filter with good
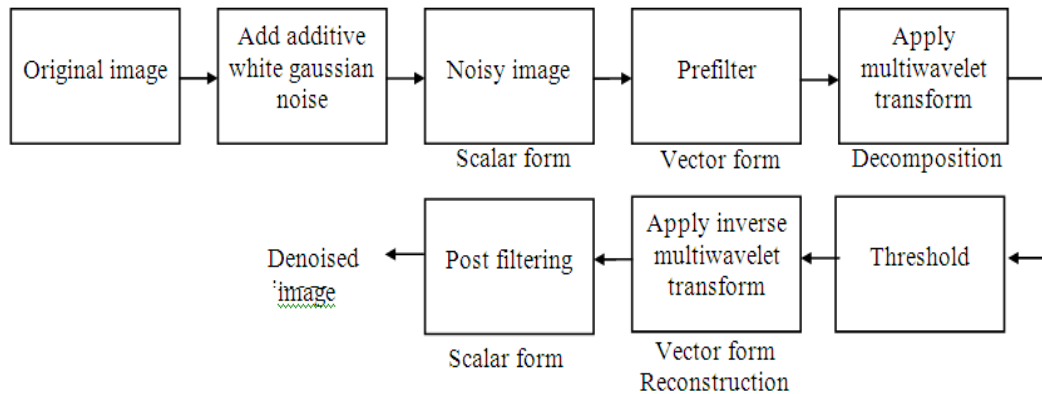
energy compaction properties can decorrelate a fairly uniform input signal into a small number of scaling coefficients containing most of the energy and a large number of sparse wavelet coefficients, typically represented with significantly fewer bits on average than the scaling coefficients.

5. Multiwavelets require roughly twice as much computation as wavelets. But multiwavelets can give performance comparable to wavelets. With short filters with length half that of wavelet filters. Thus, for the same quality of decomposed levels, multiwavelets requires about half the number of operations.

Implementation

The proposed new sub-band adaptive Bivariate shrinkage is applied to denoise a tomographic image (phatom) using multiwavelet transform and is compared with other thresholding techniques such as Universal threshold, Modified universal threshold, multivariate threshold, using various multiwavelet transforms such as GHM, CL, SA4, BiH52S, CARDBAL2 using repeated row preprocessing. The measuring parameters used are MSE and SNR.
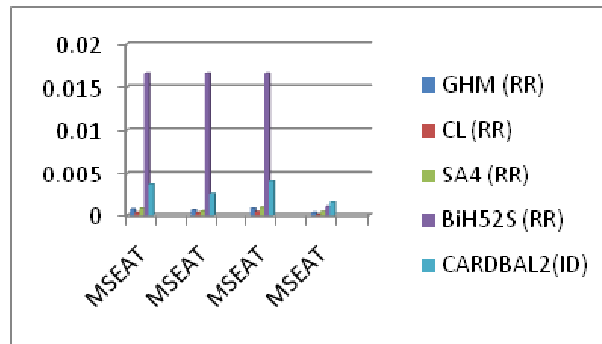

Figure 9: Block diagram of denoising an image.

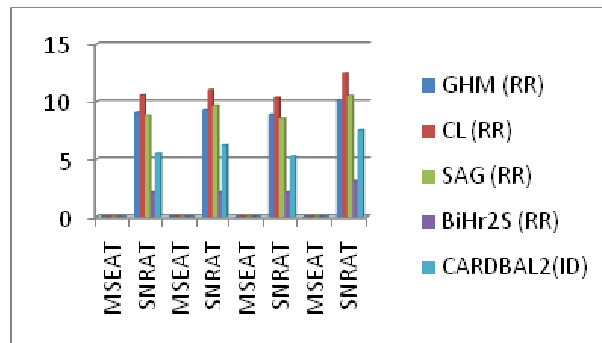**Table 1:** Denoising results using various multiwavelet & thresholding techniques.

S.No	Type of MW transform	Universal Threshold		Modified Universal Threshold		Multivariate Threshold		Proposed bivariate shrinkage	
		MSEAT	SNRAT	MSEAT	SNRAT	MSEAT	SNRAT	MSEAT	SNRAT
1.	GHM (RR)	0.0007	9.0868	0.0006	9.3049	0.0008	8.8947	0.0003	10.1536
2.	CL (RR)	0.0003	10.6101	0.0003	11.0779	0.0004	10.3887	0.0001	12.5279
3.	SAG (RR)	0.0008	8.8167	0.0005	9.6747	0.0009	8.5585	0.0004	10.5347
4.	BiHr2S (RR)	0.0166	2.1936	0.0166	2.1886	0.0166	2.1896	0.0010	3.1516
5.	CARDBAL2(ID)	0.0036	5.5377	0.0025	6.2752	0.0040	5.2826	0.0015	7.5728

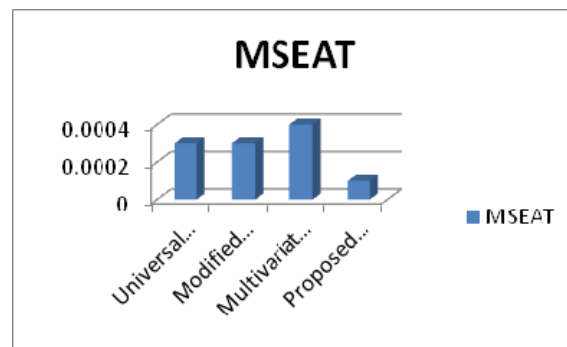**Table 2:** Denoising using GHM MWT and various thresholding technique.

S.No	Types of thresholding technique	CL	
		MSEAT	SNRAT
1.	Universal Threshold	0.0003	10.6101
2.	Modified Universal Threshold	0.0003	11.0779
3.	Multivariate Threshold	0.0004	10.3887
4.	Proposed bivariate shrinkage	0.0001	12.5279

Figure 10a

Figure 10b

Figure 11a

Figure 11b

Figure 12

Noisy Phantom
Image

Denoised
Phantom image
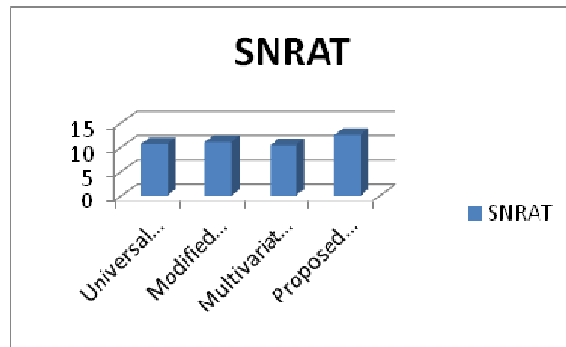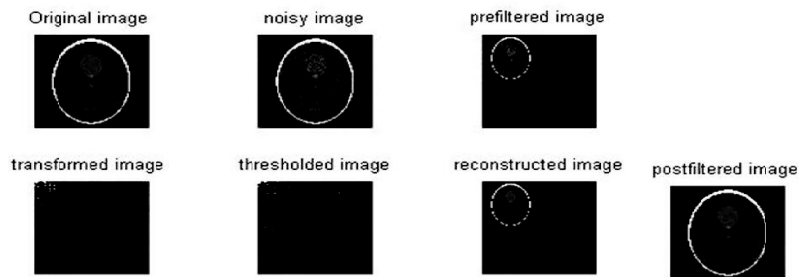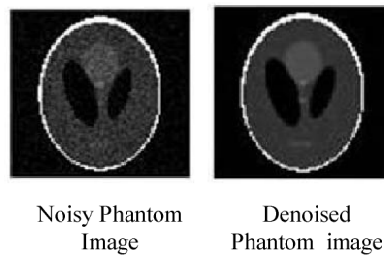
Figure 13

Conclusion

There are a number of wavelet based thresholding techniques, with which denoising of an image has been done by various researchers. As multiwavelets have advantage over wavelets and in combination with newly proposed Bivariate shrinkage, the results obtained are comparably better than the existing thresholding techniques.

It is observed from our results that CL multiwavelets with Bivariate shrink are gave better results.

Future Scope

Inspite of a number of applications of denoising techniques, the researchers could not

be able to achieve 100% noise free image. So, there is a lot of research scope in this field.

References

[1]   D.L. Donoho and I.M. Johnstone, "Ideal spatial adaptation vai wavelet shrinkage," Biometrika, vol. 81, pp.425-455, 1994.

[2]   S.G. Chang, B.Yu, and M. Vetterli, "Adaptive wavelet thresholding for image denoising and compression, "IEEE trans. Image Processing, vol. 9, pp. 1532-1546, Sept. 2000.

[3]   M.K. Mihcak, I, Kozintsev, K. Ramchandran, and P.Moulin, "Low-complexity image denoising based on statistical modeling of wavelet coefficients, "IEEE Signal Processing Lett., vol. 6, pp. 300-303, Dec. 1999.

[4]   Z. Cai, T.H. Chang, C. Lu, and K.R. Subramanian, "Efficient wavelet based image denoising algorithm,"Electron Lett., vol. 37, no. 11, pp. 683-685, May 2001.

[5]   L. Sendur and I.W. Selesnick, "A bivariate shrinkage function for wavelet based denoising," in IEEE ICASSP, 2002.

[6]   T.N.T. Goodman and S.L. Lee, "Multiwavelets of Multiplicity r", Tr. Am. Math. Soc., Vol. 342, pp. 307-324, 1994.

[7]   J. Geronimo, D. Hardin and P.R. Massopust, "Fractal Functions and Wavelet Expansions Based on Several Functions", J. Approx. Theory, Vol. 78, pp. 373-401, 1994.

[8]   C.K. Chui and J.A. Lian, "A study of Orthonormal Multiwavelets", Texas A&M.U CAT Report, No. 351, 1995.

[9]   L.X. Shen, H. H. Tan, and J. Y. Tham, "Symmetric-antisymmetric Orthonormal Multiwavelets and related Scalar Wavelets", 1997, http://citeseer.nj.nec.com/cs.

[10] V. Strela and A.T. Walden, "Denoising vis Wavelet Shrinkage: Orthogonal, Biorthogonal and Multiple Wavelet Transforms", T. Report, Impleraial College of Science, UK, 1998.

[11] T.R. Downie and B.W. Silverman, "The Discrete Multiple Wavelet Transform and Thresholding Methods", IEEE Transac. On Signal Processing, Vol, 46, pp. 2558-2561, 1998.

[12] D.L. Donoho and I.M. Jonhston, "Adapting to Unkown Smoothness Via Wavelet Shrinkage", J American Statist. Assoc., Vol. 90, pp. 1200-1224, 1995.

[13] Selesnick, "Multiwavelet Baes with Extra Approximation Properties", 1998, http://citeseer.nj.nec.com/cs.

[14] X.G. Gia, "A New Prefiler Design for Discrete Multiwavelet Transforms". IEEE Transactions on Signal Processing, Vol. 46, No. 6, pp. 1558-1570, 1998.

[15] X.G. Xia, J.S. Geronimo, D.P. Hardin and B.W. Suter, "Design of Prefilters for Discrete Multiwavelet Transforms", IEEE Trans. on Signal Processing, Vol. 44, pp. 25-35, 1996.